Modelling the transient emission from a twin conductor cable

Ian Brook Darney

Retired, Bristol, UK
E-mail: iandarney@blueyonder.co.uk

Published in *The Journal of Engineering*; Received on 11th December 2015; Accepted on 14th December 2015

Abstract: Using the equations of transmission line theory, a programme is developed to simulate the response of an open-circuit line to a step pulse. This is compared with the observed response of a twin-conductor cable. It is deduced that not all of the current delivered to the send conductor arrives back via the return conductor. Some of it departs in the form of radiated emission. A virtual capacitor is used to simulate this, with limited success. However, by adding a second virtual capacitor to simulate transient current being delivered from the return conductor back to the send conductor, a fair correlation is achieved between theoretical and actual results. This analysis demonstrates that the return conductor plays an active role in propagating any signal along the cable. This study also demonstrates that a circuit model can be created to simulate the mechanisms involved in the radiation of interference from power supply cables. This is but one example of the use of circuit models to analyse electromagnetic interference (EMI). The key relationship between electromagnetic theory and circuit theory which enables this technique to be used to analyse any EMI problem is identified. A dramatic simplification in the mathematics can be achieved.

1 Introduction

To understand the mechanisms involved the propagation of electromagnetic interference (EMI), it is necessary for the circuit designer to have a basic understanding of how electromagnetic fields relate to the performance of the equipment-under-review. This can be done without invoking the complex mathematics usually associated with the subject.

The starting point of this paper is a brief summary of the analysis of the half-wave dipole. When this antenna is driven at its resonant frequency, it delivers current into the environment. That is, it emits a stream of charged particles from every point on the conducting surface. These charges radiate away at near-light velocity.

In textbooks on electromagnetic theory, the final section on transmission lines usually deals with the transient behaviour when a step pulse is applied. Currents and voltages propagate in both directions along each conductor, and are reflected at both terminations. This mechanism is modelled here by a simple programme which allows the transient response of the line to be simulated, whatever the input waveform. This is achieved by representing current as a flow of discrete charges.

To analyse the behaviour of a lossy line, it was necessary to observe the response of an actual setup. The transient response displayed on the screen of an oscilloscope provided a template. The task then was to modify the basic model to enable it to replicate that response. There can be no better guidance than that provided by the performance of real hardware.

When a step pulse is applied via a low resistance to a lossless cable which is open circuit at the far end, the resultant current is a square pulse of gradually decreasing amplitude. That is as far as books on theory take us. The actual waveform in a twin-conductor cable is a square waveform, gradually morphing into a sine wave at a slightly lower frequency. Assessing this waveform provided clues as to how to proceed.

The first observation was that the first trailing edge seemed to follow an exponential decay. This was because the current in the send conductor was radiating away into the environment. At the leading edge of the first transit, none of the current departing from the near end actually arrived at the far end. By inserting a virtual capacitor into the model, this effect could be simulated.

There were still notable differences between the theoretical and actual responses. It was eventually reasoned that the antenna-mode current propagates faster than the differential-mode current. Therefore, the send conductor acts as a transmitting antenna. Since the return conductor was routed alongside, it was behaving as a transmitter as well as a receiver. It delivered most of the forward current back toward the near end. Inevitably, some of that backward-flowing current was lost to the environment. However, a fraction of that lost current arrived back at the send conductor. This effect was simulated by adding another virtual capacitor to the model, and this resulted in a much improved resemblance to the actual waveform.

It was then noted that, the smaller the values of the virtual capacitors became, the more closely did the response of the model correlate with the zero-loss model. This led to the conclusion that, as the step pulse progressed, half the charge was transferred to the return conductor, creating a current flow back to the near end. In turn, this transient flow delivered charge back to the send conductor.

There was a continuous flow of charges into and out of the surface of each conductor. If the current flow in one direction is equal to a current flow in the opposite direction, the nett current flow is zero, but the voltage between the conductors is doubled. This continuous interchange of charges between the conductors ensures that the nett flow of energy along the cable follows the path of the cable.

Since the return conductor plays an active role in creating the differential-mode current and in steering the electromagnetic energy along the cable from source to load, it is both misleading and unnecessary [1] to depict that conductor as an equipotential surface.

The test and analysis described in the following pages can be carried out by any final-year student of electrical engineering or by any electronic equipment designer in the workplace.

2 Half-wave dipole

The analysis of the half-wave dipole as a transmitter assumes that a sinusoidal current is delivered to the two monopoles [2], as illustrated by Fig. 1*a*.

Current in the small segment dz will create a magnetic potential at point P. Formulae for the magnitude of this potential can be calculated using three-dimensional vector analysis, using spherical co-ordinates. Formulae can then be derived for the components of the magnetic field vector $\boldsymbol{H}$ and the electric field vector $\boldsymbol{E}$ at that

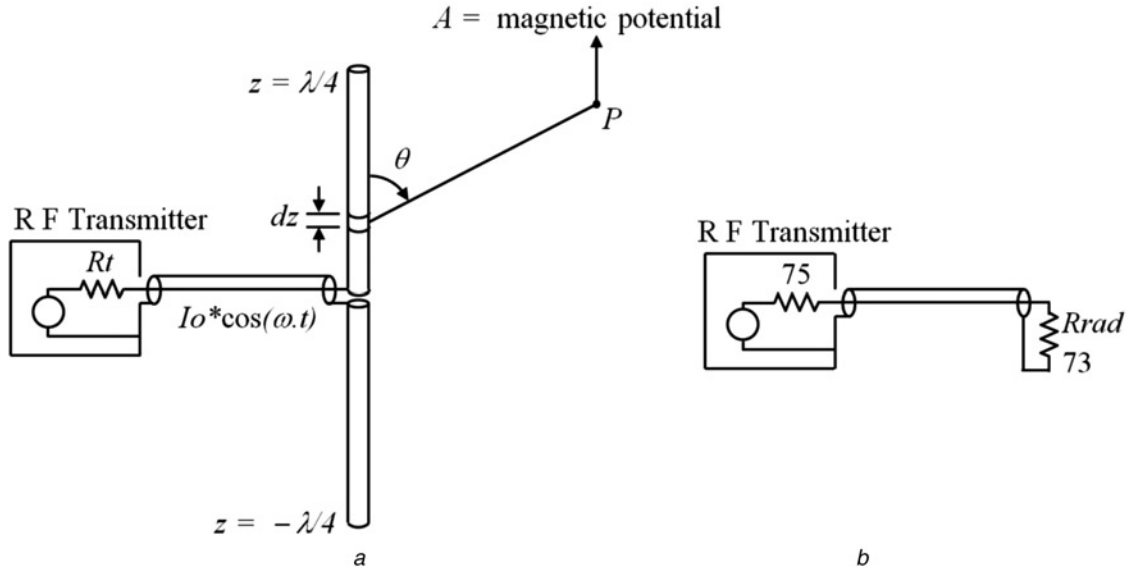

Fig. 1 *Relating a circuit model to a transmitting dipole*
a Emission from a half-wave dipole
b Circuit model when dipole is operating at resonant frequency

point. It is reasoned that the only components of the total field which are capable of propagating power away from the antenna are due to the latitudinal component of the *E*-field and the longitudinal component of the *H*-field. The product of these two components gives a formula for the power density *S* at the point *P*.

Integrating this function over the entire surface of the sphere gives an expression for the total radiated power, P_{tot}

$$P_{\text{tot}} = \frac{1}{2} \cdot R_{\text{rad}} \cdot I_o^{\,2} \tag{1}$$

where I_o is the current delivered to the antenna at its resonant frequency and R_{rad} is a parameter defined as the radiation resistance. This leads to the circuit model of Fig. 1*b*.

Comparing Figs. 1*a* and *b*, it is evident that current must flow axially along the length of each monopole and radially out of the surface to create the electromagnetic field which radiates outwards. Effectively, it is current which is departing into the environment.

This visualisation is entirely compatible with the concept of skin effect [3], where the current density becomes much higher at the conductor surface as the frequency increases.

3 Modelling a lossless line

3.1 Charge propagation

Transmission line theory introduces the concept of a pulse which propagates along the length of a transmission line at a velocity comparable with the speed of light in vacuo [4]. If a step voltage *V* is applied to the input terminals, then a step current *I* will be created. The current and voltage steps will propagate in synchronism [5].

The relationship between voltage *V* and current *I* is

$$V = R_o \cdot I \tag{2}$$

where R_o is the characteristic resistance of the line. The term 'impedance' is not used here because there is no phase difference between the voltage and the current. If there is no phase difference, the concept of impedance becomes misleading.

If the line is visualised as being made up of a number of segments of equal length, then a charge *Q* will flow into the first segment during a time d*t*, where

$$Q = I \cdot \mathrm{d}t \tag{3}$$

(In this context, the parameter d*t* is assumed to be finite.) During the next time period d*t*, this charge will flow into the second segment and a further charge *Q* will flow into the first segment. This process will continue until the charge arrives at the far end of the line. If the length of the line is *len* and the velocity of propagation is *v*, then the time *T* taken for this to happen will be

$$T = \frac{len}{v} \tag{4}$$

If there are *n* segments, then the time taken to propagate along one segment will be d*t*

$$\mathrm{d}t = \frac{T}{n} \tag{5}$$

Since R_o and *T* have been derived from the inductance and capacitance of the line, it is possible to calculate values for the loop inductance L_a and the inter-conductor capacitance C_a [6]

$$L_a = T \cdot R_o \tag{6}$$

$$C_a = \frac{T}{R_o} \tag{7}$$

Equations (6) and (7) can be used to relate analyses in the frequency domain to those in the time domain.

The function *forward*(***F***, *Qn*), defined on the Mathcad worksheet of Fig. 2, simulates the propagation of charge along the line. The input parameters are ***F***, a vector of $n+2$ elements and Q_{n}, the charge delivered to the near end of the line during time d*t*. The function moves each charge one segment forward. The output is ***F***, the updated vector and Q_{f}, the charge arriving at the far end of the line at time *T*. The process is similar to the action of a shift register.

3.2 Reflections

To deal with the response at the far end of the line, transmission line theory introduces the concept of partial currents and partial voltages. Simulating the behaviour of these parameters requires that each be uniquely identified:

doi: 10.1049/joe.2015.0193

Basic Model. SI units are used for all parameters.

$Ro := 100 \qquad Vg := 100 \qquad Rg := 10 \qquad RL := 100 \cdot 10^{6}$

$n := 100 \qquad T := 100 \cdot 10^{-9} \qquad dt := \frac{T}{n} = 1 \times 10^{-9}$

$$near(Ini, Vg) := \begin{vmatrix} Ina \leftarrow \frac{2 \cdot Ro \cdot Ini + Vg}{Ro + Rg} \\ Inr \leftarrow Ina - Ini \\ (Inr \quad Ina) \end{vmatrix} \qquad far(Ifi) := \begin{vmatrix} Ifa \leftarrow \frac{2 \cdot Ro \cdot Ifi}{Ro + RL} \\ Ifr \leftarrow Ifa - Ifi \\ (Ifr \quad Ifa) \end{vmatrix}$$

$$forward(\boldsymbol{F}, Qn) := \begin{vmatrix} \boldsymbol{F}_1 \leftarrow Qn \\ \text{for } x \in n+1 \,..\, 1 \\ \quad \boldsymbol{F}_{x+1} \leftarrow \boldsymbol{F}_x \\ Qf \leftarrow \boldsymbol{F}_{n+2} \\ (\boldsymbol{F} \quad Qf) \end{vmatrix} \qquad back(\boldsymbol{B}, Qf) := \begin{vmatrix} \boldsymbol{B}_{n+1} \leftarrow Qf \\ \text{for } x \in 2 \,..\, n+1 \\ \quad \boldsymbol{B}_{x-1} \leftarrow \boldsymbol{B}_x \\ Qn \leftarrow \boldsymbol{B}_1 \\ (\boldsymbol{B} \quad Qn) \end{vmatrix}$$

$N := 10 \cdot n - 1 \qquad i := 1 \,..\, N \qquad \boldsymbol{t}_i := i \cdot dt$

$$\boldsymbol{Ina} := \begin{vmatrix} \boldsymbol{F}_{n+2} \leftarrow 0 \\ \boldsymbol{B}_{n+1} \leftarrow 0 \\ \text{for } i \in 1 \,..\, N \\ \quad \begin{vmatrix} Vgen \leftarrow Vg \quad \text{if } i > 1 \\ (Inr \quad Ina) \leftarrow near(Ini, Vgen) \\ (\boldsymbol{F} \quad Ifi) \leftarrow forward(\boldsymbol{F}, Inr) \\ (Ifr \quad Ifa) \leftarrow far(Ifi) \\ (\boldsymbol{B} \quad Ini) \leftarrow back(\boldsymbol{B}, Ifr) \\ \boldsymbol{A}_i \leftarrow Ina \end{vmatrix} \\ \boldsymbol{A} \end{vmatrix}$$

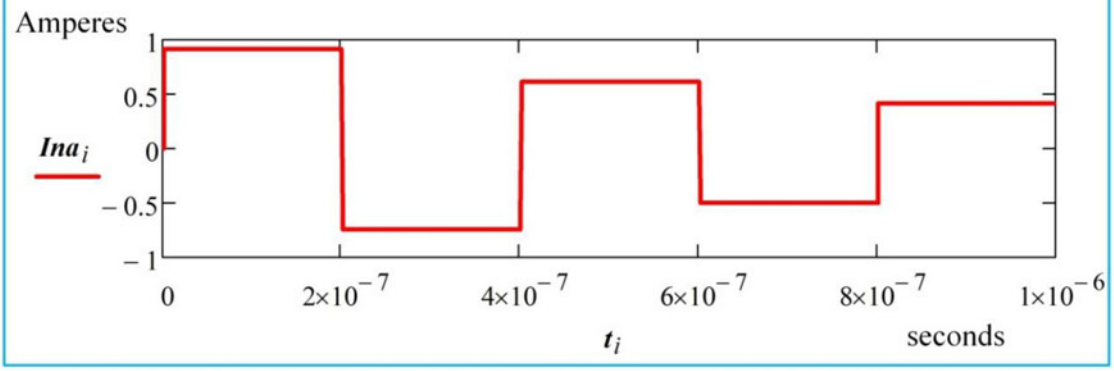

Fig. 2 *Response of a lossless open-circuit line to a step voltage input*

doi: 10.1049/joe.2015.0193

V_{fi} and I_{fi} are the incident voltage and incident current at the far end.
V_{fr} and I_{fr} are the reflected voltage and reflected current at the far end.
V_{fa} and I_{fa} are the voltage and current absorbed at the far end.

These can be related

$$V_{fi} + V_{fr} = V_{fa} \tag{8}$$

$$I_{fi} + I_{fr} = I_{fa} \tag{9}$$

$$V_{fi} = R_o \cdot I_{fi} \tag{10}$$

$$V_{fr} = -R_o \cdot I_{fr} \tag{11}$$

$$V_{fa} = R_L \cdot I_{fa} \tag{12}$$

where R_L is the resistance of the load at the far end.

The parameters at the near end are identified in a similar way. For example, V_{ni} and I_{ni} are the incident voltage and incident current at the near end.

Subtracting (11) from (10) and invoking (9) gives

$$V_{fi} - V_{fr} = R_o \cdot (I_{fi} + I_{fr}) = R_o \cdot I_{fa} \tag{13}$$

Adding (8) and (13) and invoking (10) gives

$$2 \cdot R_o \cdot I_{fi} = R_L \cdot I_{fa} + R_o \cdot I_{fa}$$

This leads to

$$I_{fa} = \frac{2 \cdot R_o \cdot I_{fi}}{R_L + R_o} \tag{14}$$

This means that, given a value for I_{fi}, I_{fa} can be calculated. Then I_{fr} can be calculated using (9). This leads to the Mathcad function *far*(I_{fi}), defined on the worksheet of Fig. 2.

From (3), the value of the incident current I_{fi} is proportional to the charge Q_{fi} arriving at the far end. That is, $I_{fi} = (Q_{fi}/dt)$. The function *far*(I_{fi}) takes as input the value of I_{fi} and provides the values of I_{fr} and I_{fa} as output. The reflected current I_{fr} delivers a charge $Q_{fr} = I_{fr} \cdot dt$ to the line and this charge propagates back to the near end. The function *back*(***B***, Q_f), defined in Fig. 2, simulates this action.

At the near end, this charge manifests itself as the current I_{ni}, where $I_{ni} = (Q_{ni}/dt)$. Since there is a voltage source V_g at this end, the relationship between the voltages is

$$V_{ni} + V_{nr} + V_g = V_{na} \tag{15}$$

The other relationships are basically those of (9)–(12). This leads to the function *near*(I_{ni}, V_g), defined in Fig. 2. This function takes the instantaneous values of V_g and I_{ni}, and uses them to calculate the values of I_{nr} and I_{na}.

3.3 Basic delay line model

The worksheet of Fig. 2 shows how these functions can be used to simulate the response of a lossless line.

The constants are set out at the top of the page. The value of the characteristic resistance R_o is 100 Ω, the step voltage V_g delivered by the generator is 100 V, the output resistance R_g of the voltage source is 10 Ω, the resistance of the load R_L at the far end is set at 100 MΩ, (effectively an open circuit) the number n of line segments is set at 100, and it is assumed that the time constant, T, is 100 ns. This means that the time taken to propagate along the length of a single segment is 1 ns.

Then the four functions are defined and the number of reflections, N, is set at ten. This allows the control variable i and the time vector $\boldsymbol{t}_i$ to be defined.

The first action of the main programme is to define the vectors ***F*** and ***B***. Vector ***F*** records the value of the forward-moving charge on each segment at any particular instant. The vector ***B*** holds the values of the backward-moving charges.

The iterative section of the programme assumes that the initial value of I_{ni} is zero and assigns the value of 100 to V_{gen}. In Mathcad, the variables which are defined outside the main programme are visible inside the programme, but those inside the programme are invisible outside.

The control variable i is set to carry out N iterations. For each iteration, the function *near*(I_{ni}, V_{gen}) calculates a value for I_{nr}. Each function uses the output of the preceding function to provide an input to the succeeding function. The vector ***A*** then stores the value of the selected variable at that instant, in this case, I_{na}. After all the iterations have been completed, the contents of the vector ***A*** are stored by the vector $\boldsymbol{I}_{na}$.

Then the graph plots the amplitude of the input current $\boldsymbol{I}_{na}$ against the time ***t***. In this worksheet, both the calculations and the graphical results are displayed on this one page.

4 Testing

4.1 Test setup

The worksheet of Fig. 2 now forms a foundation on which further development can be based. It simulates the action of the delay-line model of Fig. 3*a*. However, the only guidance available on how to simulate a lossy line lay with an examination of the actual performance of such an assembly. Fig. 3*b* illustrates a setup used to do just that.

The assembly-under-test was a 15 m length of twin-conductor mains cable, open circuit at the far end, and the instrumentation was an oscilloscope and a signal generator. An interface box was built, to provide a low resistance source of ∼9 Ω to drive the cable. With a low resistance at the near end and an open-circuit at the far end, multiple reflections were guaranteed. Such a response

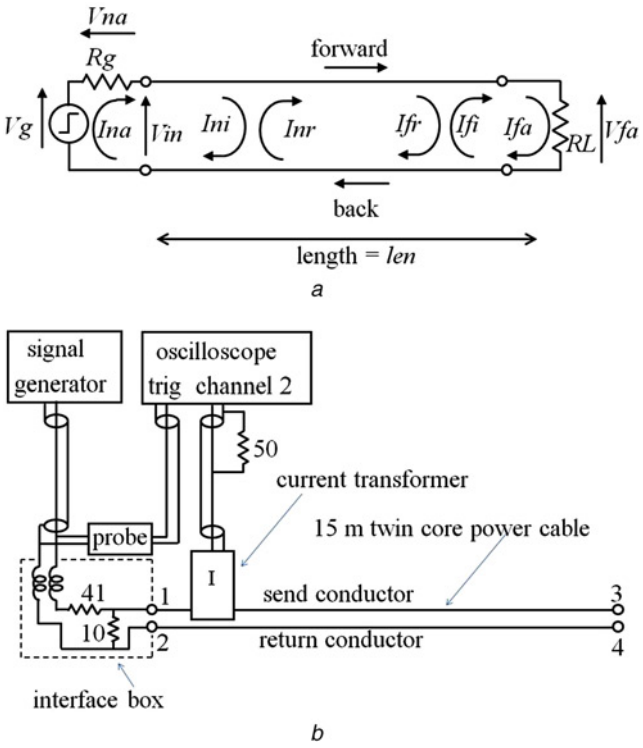

Fig. 3 *Relating the circuit model to the assembly-under-review*
a Delay-line model of a lossless transmission line
b Test setup used to measure the performance of a lossy line

doi: 10.1049/joe.2015.0193

allowed a great deal of information to be gleaned from the observed waveforms.

The 41 Ω resistor and the 10 Ω resistor provided a potential divider which minimised the interaction between the cable input and the signal generator. A common-mode choke was also installed at this interface to introduce an inductance between the ground conductors of the test equipment and the cable. This consisted of a bi-filar winding of 14 turns of 22 standard wire gauge enamelled copper wire on a Maplin N88 ferrite core. Over the range of frequencies involved in the tests, the inductance of this device acted as a high impedance between the instrumentation and the cable.

This setup ensured that there would be minimal current flow between the earthed conductors of the test equipment and the return conductor of the cable-under-test; at least, no current flow which affected the transient response. The only path for cable current to take was along the send conductor and back via the return conductor.

4.2 Test procedure

A square waveform of about 100 kHz was applied between terminals 1 and 2 at the near end of the cable. Such a choice of frequency allowed the reverberations following each step to die down before the next step was applied. The current in the line was monitored by a current transformer and the monitored waveform displayed on an oscilloscope. Details of construction and calibration of this device are provided in [7]. To ensure reliable triggering of the displayed waveform, a times-ten voltage probe was connected to the input terminals of the interface box. Fig. 4 is a copy of one photograph taken of the display on the screen of the oscilloscope.

4.3 Scaling

The task now was to modify the delay-line model of Fig. 2 to replicate the actual response, as defined by Fig. 4. Examination of this waveform provided data which allowed values to be assigned to the constants in the delay-line model. Fig. 5 provides the details. Plugging these values into the basic delay-line model resulted in a waveform which is replicated by Fig. 6*a*. This is essentially the same as the graph in Fig. 2, but with the appropriate scaling for the assembly-under-test.

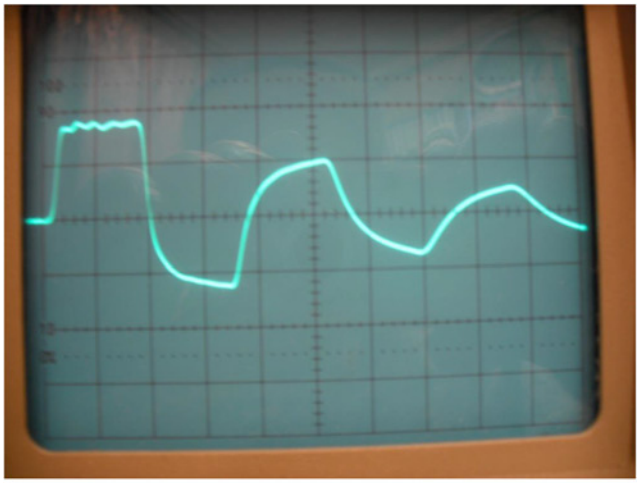

Horizontal scale – 100 ns/div. Vertical scale – 10 mV/div

Fig. 4 *Waveform of transient current at the input of an open-circuit cable*

5 Analysis

5.1 Current flow

The setup of Fig. 3*b* included a common-mode choke to ensure that there was no current flow from the earthed conductors of the test instruments into terminal 2 of the cable. If the output voltage of the generator was positive, current would flow through the 41 Ω resistor, terminal 1, the send conductor, across the gap between the cable conductors, then back through the return conductor, terminal 2, the common-mode choke, the screen of the co-axial cable, and finally to the return terminal of the output driver in the signal generator. There is no way of avoiding the conclusion that current must flow across the gap between the cable conductors.

The velocity of propagation of the pulse along the cable can be calculated from the measured values of time and length

$$v = \frac{len}{T} = \frac{15}{8.25 \times 10^{-8}} = 182 \text{ m/}\mu\text{s} \tag{16}$$

Such a velocity precludes the concept that this flow of current is carried by electrons or protons. Therefore, it is reasonable to conclude that sub-atomic particles are involved. The name given by the scientific community to such entities is ‘photons’. A photon is an elementary particle, the quantum of light and all other forms of electromagnetic radiation [8].

5.2 Ideal response

The analysis leading to the creation of the waveform of Fig. 6*a* can be visualised in greater detail. A step voltage V_{in} applied to terminal 1 will cause a current I_{nr} to flow into the first segment of the send conductor. This current flow will deliver a charge Q. Charge then flows across the gap and delivers a charge $-Q/2$ to the return conductor, leaving a charge $Q/2$ on the send conductor. This charge on the return conductor will flow back to terminal 2. The net result is a current flowing along the send conductor and back along the return conductor. Since the current in this loop has changed from zero to I_{nr} in time dt, a voltage will be developed along both conductors, due to inductive effects.

After time dt, a step voltage V_{nr} will arrive at the second segment, and the process will continue. After a time T, the step will arrive at the far end, with a charge $Q/2$ having been delivered to every segment of the send conductor and a charge $-Q/2$ being delivered to the segments of the return conductor. Then the forward motion ceases. There is no longer a flow of charge into the return conductor. Therefore, the charge in the final segment of the return conductor flows back into the send conductor, creating a charge Q in the final segment of that conductor. This process means that the return conductor discharges into the send conductor during the entire time the step is propagating back toward the near end.

5.3 Actual response

Having created a visualisation of the ideal process, it is possible to glean an improved visualisation from an assessment of the actual waveform.

The rounded corners and the finite rise-time of the leading edge of the waveform of Fig. 4 are probably due to the differential-mode inductance and capacitance of the common-mode choke and to the limited bandwidth of the current transformer. The ripple on top of the waveform during the following 150 ns is probably due to discontinuities at either end of the common-mode choke. The period between the rising and trailing edges is a measure of the time taken for the current step to propagate to the far end of the cable, be reflected, and to propagate back to arrive as incident current at the near end.

However, the slow decay of the first trailing edge cannot be ascribed to imperfections in the test equipment. This part of the waveform is due to the first reflection at the near end. If this end

Test Data SI units are used for all parameters

Vertical scaling

$Vch2 := 17 \cdot 10^{-3}$ *Vch2* = Amplitude of first step in the voltage waveform, as monitored by channel 2 of the oscilloscope. See Figure 4

$RT := 2.27$ *RT* = Transfer resistance: The ratio between the amplitude of the voltage monitored on Channel 2 of the scope to the current *Imon* flowing in the conductor-under-test. See reference [6].

$Imon := \frac{Vch2}{RT} = 7.489 \times 10^{-3}$ The differential-mode current flowing in the cable.

$Vin := 0.84$ Amplitude of the voltage step at input terminals, as monitored by a voltage probe. See Figure 3(a)

$Ro := \frac{Vin}{Imon} = 112.165$ *Ro* = charactaristic resistance of the cable

$Rg := \frac{10 \cdot 91}{10 + 91} = 9.01$ Input resistance; 41+50 ohm in parallel with 10 ohm

$Vg := Vin \cdot \frac{Rg + Ro}{Ro} = 0.907$ See Figure 3(a).

Horizontal scaling

Each division of the graticule shown on Figure 4 represents 100ns. If the vertical line at the left hand side represents $t = 0$, then the time of the first rising edge $T1$, is 20ns and the time $T2$ of the final graticule line is 1000ns. So:

$T1 := 20 \cdot 10^{-9}$

$T2 := 1000 \cdot 10^{-9}$

$T := \frac{(185 - 20) \cdot 10^{-9}}{2} = 8.25 \times 10^{-8}$ 2**T* = time between initial rising edge and initial falling edge: See Figure 4.

$n := 100$ Number of segments of the line.

$dt := \frac{T}{n} = 8.25 \times 10^{-10}$ The time taken to propagate along one segment

$N1 := floor\left(\frac{T1}{dt}\right) = 24$ Number of time steps at which step input voltage occurs

$N2 := floor\left(\frac{T2}{dt}\right) = 1212$ Number of time steps corresponding to 1000 nanoseconds

Fig. 5 *Deriving values for the constants*

had been a short circuit, the reflected current would have been double the amplitude and opposite in sign to the incident current. Since the resistance R_g is small, but finite, the amplitude of the reflected current is slightly less. Since the generator continues to supply constant current, the effect is to create a reflected current with a lower amplitude, but opposite in sign, to the incident current. This means that the waveform of the current I_{na} at time $2 \cdot T$ provides an inverted, amplified, picture of the current waveform which had arrived at the far end at time T.

Since this waveform is similar to the exponential rise in the voltage delivered to an R–C circuit, it is reasonable to surmise that current is departing into the environment via capacitive

doi: 10.1049/joe.2015.0193

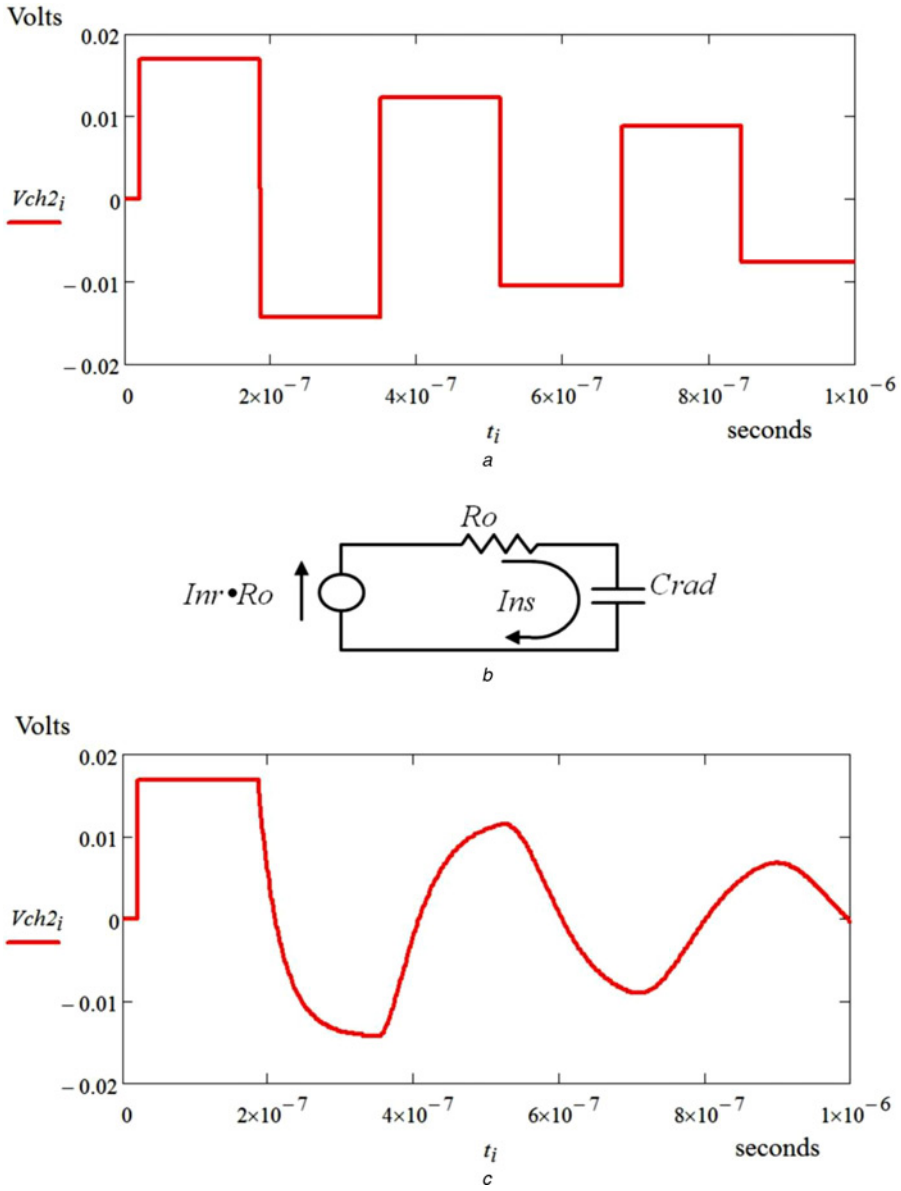

Fig. 6 *Developing the basic model to enable it to simulate transient emissions*
a Response of the setup of Fig. 3*b*, assuming no losses
b Circuit model which simulates current loss to the environment
c Simulated waveform, assuming current loss to the environment

coupling and that the current arriving at the far end is that which has not departed. As the leading edge propagates along the cable, current flows radially outwards as well as axially along the length. Fig. 6*b* is a circuit model which simulates this current.

Assuming that the value of the capacitor is C_{rad} and that the current delivered to the environment is I_{ns}, then

$$V_{\text{nr}} = R_o \cdot I_{\text{nr}} = R_o \cdot I_{\text{ns}} + \frac{Q_{\text{ns}}}{C_{\text{rad}}} \tag{17}$$

giving

$$I_{\text{ns}} = I_{\text{nr}} - \frac{Q_{\text{ns}}}{R_o \cdot C_{\text{rad}}} \tag{18}$$

With time-step analysis, the initial value of Q_{ns} can be stored and used to calculate the initial value for I_{ns}. Then the new value for Q_{ns} can be calculated using the Mathcad expression

$$Q_{\text{ns}} \leftarrow Q_{\text{ns}} + I_{\text{ns}} \cdot \mathrm{d}t \tag{19}$$

Since I_{ns} is the current lost to the environment, the current actually delivered to the next segment, I_{nt}, will be

$$I_{\text{nt}} = I_{\text{nr}} - I_{\text{ns}} \tag{20}$$

This leads to the Mathcad function *discharge*(I_{nr}, Q_{ns}) defined in the worksheet of Fig. 7. This function takes the values of the reflected current I_{nr} and the previous value of Q_{ns}, uses them to calculate the amplitude of the current radiating out into the environment I_{ns}, the current transmitted to the next segment I_{nt}, and the updated value of Q_{ns}. Then it provides values for these three variables as output. Modifying the worksheet of Fig. 2 to simulate this current loss leads to the waveform of Fig. 6*c*.

This waveform is much more representative of the actual behaviour of the cable than the response of the basic delay-line model;

Recharge. Page 1 of Worksheet

$Vg := 0.9 \qquad Ro := 112 \qquad Rg := 9 \qquad RL := 100 \cdot 10^{6}$

$T := 82.5 \cdot 10^{-9} \qquad n := 100 \qquad dt := \frac{T}{n}$

$Crad := 280 \cdot 10^{-12}$ Radiating capacitor: Select-on-test constant.

$Cret := 100 \cdot 10^{-12}$ Recharging capacitor: Select-on-test constant.

$$near(Ini, Vg) := \left| \begin{array}{l} Ina \leftarrow \frac{2 \cdot Ro \cdot Ini + Vg}{Ro + Rg} \\ Inr \leftarrow Ina - Ini \\ (Inr \quad Ina) \end{array} \right.$$

$$discharge(Inr, Qns) := \left| \begin{array}{l} Int \leftarrow \frac{Qns}{Ro \cdot Crad} \\ Ins \leftarrow Inr - Int \\ Qns \leftarrow Qns + Ins \cdot dt \\ (Int \quad Ins \quad Qns) \end{array} \right.$$

$$forward(\boldsymbol{F}, Int) := \left| \begin{array}{l} \boldsymbol{F}_1 \leftarrow Int \\ for \quad x \in n+1 \,..\, 1 \\ \quad \boldsymbol{F}_{x+1} \leftarrow \boldsymbol{F}_x \\ Ifi \leftarrow \boldsymbol{F}_{n+2} \\ (\boldsymbol{F} \quad Ifi) \end{array} \right.$$

$$far(Ifi) := \left| \begin{array}{l} Ifa \leftarrow \frac{2 \cdot Ro \cdot Ifi}{Ro + RL} \\ Ifr \leftarrow Ifa - Ifi \\ (Ifr \quad Ifa) \end{array} \right.$$

$$recharge(Ifr, Qfs) := \left| \begin{array}{l} Ifs \leftarrow Ifr - \frac{Qfs}{Ro \cdot Cret} \\ Qfs \leftarrow Qfs + Ifs \cdot dt \\ Ift \leftarrow Ifr + Ifs \\ (Ift \quad Ifs \quad Qfs) \end{array} \right.$$

$$back(\boldsymbol{B}, Ift) := \left| \begin{array}{l} \boldsymbol{B}_{n+1} \leftarrow Ift \\ for \quad x \in 2 \,..\, n+1 \\ \quad \boldsymbol{B}_{x-1} \leftarrow \boldsymbol{B}_x \\ Ini \leftarrow \boldsymbol{B}_1 \\ (\boldsymbol{B} \quad Ini) \end{array} \right.$$

Fig. 7 *Definition of circuit parameters and programme functions*

Fig. 6*a*. Even so, there are notable imperfections. The slope of the first trailing edge of the waveform of Fig. 6*c* is less than that of Fig. 4. Moreover, the discontinuities at the peaks of the theoretical waveform are not as sharp as those of the actual waveform.

5.4 Returning current

The reasoning above indicates that the send conductor is acting as a transmitting antenna. In fact, all of the current flowing along the send conductor during any step change in V_g radiates into the

doi: 10.1049/joe.2015.0193

Recharge. Page 2 of Worksheet

$RT := 2.27$ Transfer resistance: Ratio of *Vch2* to current in the line, *Ina*.

$T1 := 20 \cdot 10^{-9}$ $N1 := floor\left(\frac{T1}{dt}\right) = 24$ the count, *i*, at leading edge

$T2 := 1000 \cdot 10^{-9}$ $N2 := floor\left(\frac{T2}{dt}\right) = 1212$ the count, *i*, at end of sweep

$i := 1 .. N2$ $t_i := i \cdot dt$ the time variable.

$$
\begin{aligned}
&\textbf{Vch2} := \left|\begin{array}{l}
F_{n+2} \leftarrow 0 \\
B_{n+1} \leftarrow 0 \\
\text{for } i \in 1 .. N2 \\
\quad \left|\begin{array}{l}
Vgen \leftarrow Vg \quad \text{if } i > N1 \\
(Inr \quad Ina) \leftarrow near(Ini, Vgen) \\
(Int \quad Ins \quad Qns) \leftarrow discharge(Inr, Qns) \\
(F \quad Ifi) \leftarrow forward(F, Int) \\
(Ifr \quad Ifa) \leftarrow far(Ifi) \\
(Ift \quad Ifs \quad Qfs) \leftarrow recharge(Ifr, Qfs) \\
(B \quad Ini) \leftarrow back(B, Ift) \\
A_i \leftarrow Ina \cdot RT
\end{array}\right. \\
A
\end{array}\right.
\end{aligned}
$$

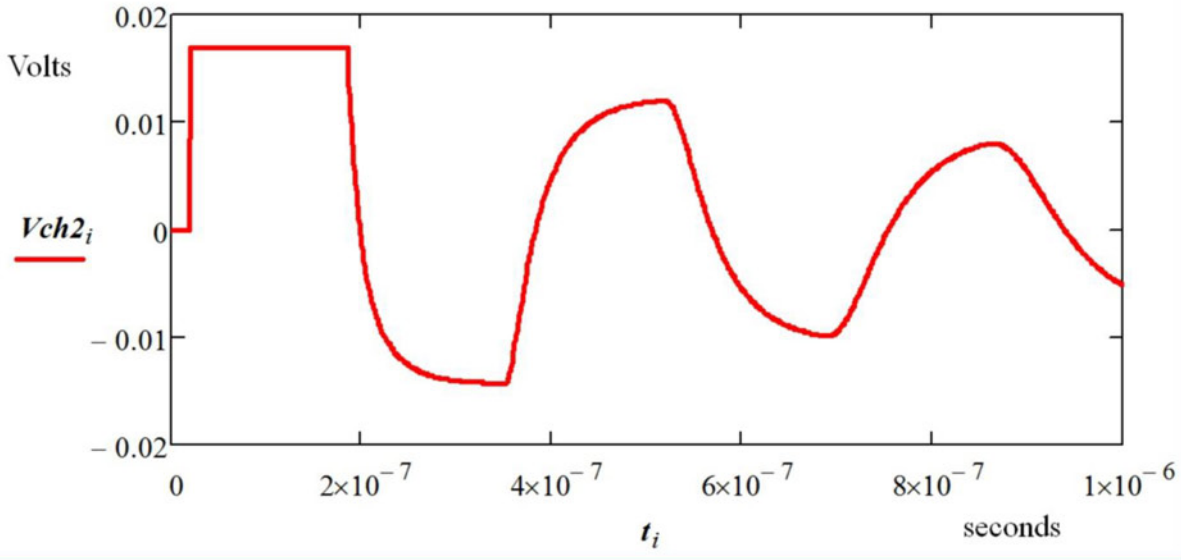

Fig. 8 *Main programme and simulated waveform*

doi: 10.1049/joe.2015.0193

environment. (Any waveform can be simulated as a series of step changes.)

At the start of the simulation, at $t = 0$, the charge Q_{ns} is zero. Substituting this value into (17) gives $I_{ns} = I_{nr}$. From (20), the current actually reaching the second segment is zero. This means that the current I_{fi} arriving at the far end at time T is zero. This is not really surprising, since the charges move at a finite velocity. It takes time to cross the gap between the two conductors.

Since the charges radiate out in all directions, most of them depart into the environment and constitute radiated interference. Some will arrive at the return conductor and will create a current in that conductor. The send conductor acts as a transmitting antenna, and the return conductor acts as a receiving antenna.

Once current flow has been established in the return conductor, it also starts to behave as a transmitting antenna. This means that some of the current it has received is delivered back to the send conductor. This action can be simulated by introducing another capacitor into the model and locating it at the far end. If this capacitor is defined as C_{ret}, a new Mathcad function can be created to simulate its action. This is defined by the function *recharge*(I_{fr}, Q_{fs}) in the worksheet of Fig. 7.

Fig. 7 is a modified version of Fig. 2, to define the constants relevant to the assembly-under-review and to include the functions *discharge*(I_{nr}, Q_{ns}) and *recharge*(I_{fr}, Q_{fs}). This modification made it necessary to spread the worksheet over two pages. The second page is illustrated by Fig. 8. The end result was a waveform which bore a much closer resemblance to that of Fig. 4 than either of the previous two simulations.

There were two unknown constants:

C_{rad}: The virtual capacitor involved in radiating current away from the send conductor into the environment.
C_{ret}: The virtual capacitor involved in coupling current back from the return conductor into the send conductor.

When the worksheet was initially formulated, guess values were assigned to these two parameters and the programme run. The resultant waveform provided information as to whether each capacitor was too large or too small. Optimum values were derived after a few iterations, and these are defined at the top of Fig. 7.

6 Assessment

6.1 Initial conclusions

The current I_{ns} in the virtual capacitor C_{rad} is a measure of the transient current that has been lost to the assembly. It simulates the radiation that is emitted.

The technique described in the previous pages can be used to measure the transient emission from any cable and to assign values to the parameters associated with that emission: T, R_o, C_{rad}, and C_{ret}. All the Mathcad worksheets used in this analysis are available for download [9]. This model caters for any input waveform and any values for the resistors at the terminations. (It can also be developed further to simulate the effect of inductors and capacitors at the terminations.)

It has been demonstrated here that circuit modelling techniques can be used to analyse EMI coupling in the time domain. There is no need to invoke the complexities of frequency-domain analysis [10].

It has also been shown that the return conductor plays an active role in the propagation of electromagnetic energy from one location to another in the system. Charge flows along the send conductor, across the gap to the return conductor, back along the return conductor, and then back to the send conductor. Current flows in a loop. It is the dynamic energy in this loop which creates the magnetic field which sustains the forward flow of electromagnetic power during the first transit. In Fig. 3*a*, I_{nr} is depicted as flowing clockwise.

At the far end, forward flow ceases. However, the static energy still exists on the final segment. Charge flows from the return conductor into the send conductor, creating an anti-clockwise flow of current; that is, I_{fr} is negative. Magnetic energy then sustains the flow of electromagnetic power during the first backward transit.

If the separation between the conductors is increased, this interchange will be impeded and the lost energy will be picked up elsewhere.

6.2 Relating the theories

Circuit theory is a simplification and development of electromagnetic theory.

The simplification which enables circuit models to be used to simulate the functional behaviour of complex assemblies is the assumption that the resistive, inductive, and capacitive properties of every conductor are zero. The benefit of such an assumption is that it allows a 'zero-volt' reference terminal to be used, enabling the model to simulate the function of complex assemblies.

The concept of the 'single-point ground' as a design guideline is well past its sell-by date. If implemented, it will guarantee maximum possible coupling between signals and power [11]. The related concept of the 'equipotential conductor' encourages equipment designers to treat the conducting structure as a convenient return path for power supplies and signals, with consequential EMI problems. This concept manifests itself in the presence of the ubiquitous earth symbol dotted around system wiring diagrams.

Since it is the interaction between conductors which causes EMI and since circuit theory is based on the assumption that conductors have zero impedance, it would appear that circuit models cannot possibly be used to simulate EMI.

However, if the circuit model is viewed in the same way as the unknown variable in mathematics, the construction of the model and the assignment of numerical values to the components can be determined by physical data derived from the assembly-under-review. This technique has been used in the past. (In the 1960s, analogue computers were used to simulate the behaviour of mechanical control systems.) It can also be invoked to simulate EMI.

The relationships of electromagnetic theory can be used to create a set of equations which define the coupling between three parallel conductors. A circuit model can be visualised which creates a similar set of equations. Correlating the two sets of equations allows the model to simulate the electromagnetic coupling mechanism [12]. Invoking the concept of distributed parameters [13], the frequency response of the model can be extended well beyond that of quarter-wave resonance. The concept of the 'virtual conductor' enables coupling between cable and environment to be simulated in the frequency domain [14]. Bench testing confirms that the technique is valid [15].

The analysis in the preceding pages demonstrates that this approach can be extended to simulate EMI in the time domain.

References [11–15] are all taken from the same book because, as far as the author is aware, no other author has followed the approach described in that book.

6.3 Misleading concepts

The concepts of the 'single-point ground' and the 'equipotential ground' are the root cause of the vast majority of EMI problems. Even so, books by leading authorities on the subject of electromagnetic compatibility (EMC) such as Ott [16], Paul [17], and Kaiser [18] continue to give credence to these concepts.

There is no such thing as a single-point ground; a zero-volt terminal to which all other voltages in the equipment can be referenced. There is no such thing as an equipotential conductor. It is

better to state these facts unequivocally than to indulge in a discussion of the relative merits of different grounding philosophies.

It is likely that discussion on the topic of 'Grounding' during the development of EMC design requirements for new vehicles, aircraft, and spacecraft is heavily influenced by the guidance provided by documents such as [16–18]. Such guidance can be invoked to support the decision to continue to use the conducting structure as a return path for power supplies and signals, and to justify the design requirement to isolate the zero-volt reference conductor in each equipment unit from the conducting structure of that unit (to eliminate ground loops).

In systems which incorporate such wiring configurations, the conducting structure behaves as an active source of EMI. Subsequent measures to mitigate the effects of interference are rather like applying first aid after the damage has been done.

6.4 Design process

On the other hand, if circuit designers are shown how to carry out bench tests on representative assemblies and to replicate the observed behaviour using circuit models, they can be empowered to make their own decisions as to the best way to design the equipment under development and to justify those decisions during formal design reviews. That is, EMC can be treated in the same way as any other design requirement.

7 Conclusion

The time has come for circuit theory to be updated to include the concepts of partial currents, partial voltages, time delays, distributed parameters, and virtual components. If this is done, system designers can achieve a much improved understanding of EMI coupling mechanisms, as well as the ability to design equipment to meet the EMC requirements using familiar analytical tools.

8 References

[1] Darney I.B.: 'The hybrid equations', in Duffy A. (Ed.): 'Circuit modeling for electromagnetic compatibility' (SciTech Publishing, Edison, NJ, 2013), pp. 273–276

[2] Skitek G.G., Marshall S.V.: 'Antennas', 'Electromagnetic concepts and applications' (Prentice-Hall, Inc., Englewood Cliffs, NJ, 1982), pp. 456–463

[3] Skitek G.G., Marshall S.V.: 'Transmission lines', 'Electromagnetic concepts and applications' (Prentice-Hall, Inc., 1982), pp. 409–411

[4] Skitek G.G., Marshall S.V.: 'Transmission lines', 'Electromagnetic concepts and applications' (Prentice-Hall, Inc., 1982), pp. 380–384

[5] Skitek G.G., Marshall S.V.: 'Transmission lines', Electromagnetic concepts and applications' (Prentice-Hall, Inc., 1982), pp. 411–413

[6] Darney I.B.: 'Transient analysis', in Duffy A. (Ed.): 'Circuit modeling for electromagnetic compatibility' (SciTech Publishing, Edison, NJ, 2013), pp. 149–150

[7] Darney I.B.: 'Bench testing', in Duffy A. (Ed.): 'Circuit modeling for electromagnetic compatibility' (SciTech Publishing, Edison, NJ, 2013), pp. 183–188

[8] Available at https://www.en.wikipedia.org/wiki/Photon, accessed October 2015

[9] Available at http://www.designemc.info/ZipMTE.zip, accessed October 2015

[10] Smith A. A.Jr.: 'Plane-wave excitation', in : 'Coupling of electromagnetic fields to transmission lines' (Interference Control Technologies, Inc., 1989), pp. 38–45

[11] Darney I.B.: 'Practical design', in Duffy A. (Ed.): 'Circuit modeling for electromagnetic compatibility' (SciTech Publishing, Edison, NJ, 2013), pp. 224–226

[12] Darney I.B.: 'Lumped parameter models', in Duffy A. (Ed.): 'Circuit modeling for electromagnetic compatibility' (SciTech Publishing, Edison, NJ, 2013), pp. 45–49

[13] Darney I.B.: 'Transmission line models', in Duffy A. (Ed.): 'Circuit modeling for electromagnetic compatibility' (SciTech Publishing, Edison, NJ, 2013), pp. 82–89

[14] Darney I.B.: 'Antenna models', in Duffy A. (Ed.): 'Circuit modeling for electromagnetic compatibility' (SciTech Publishing, Edison, NJ, 2013), pp. 107–113

[15] Darney I.B.: 'Bench testing', in Duffy A. (Ed.): 'Circuit modeling for electromagnetic compatibility' (SciTech Publishing, Edison, NJ, 2013), pp. 197–206

[16] Ott H.W.: 'Grounding', 'Noise reduction techniques in electronic systems' (John Wiley & Sons, Inc., 1988, 2nd edn.), pp. 77–88

[17] Paul C.R.: 'System design for EMC', in Chang, K., (Ed.): 'Introduction to electromagnetic compatibility' (John Wiley & Sons, Inc., 2006, 2nd edn.), pp. 796–802

[18] Kaiser K.L.: 'Grounding', 'Electromagnetic compatibility handbook' (CRC Press, 2005), pp. 28–83 to 28–85